 DOI: 10.1002/masy.200950930

Phase Behavior and Particle Formation of Poly (1H,1H-dihydrofluorooctyl Methacrylate) in Supercritical CO_2

José G. Santoyo-Arreola,[1] *Rubén C. Vásquez-Medrano,*[1] *Alberto Ruiz-Treviño,*[1] *Gabriel Luna-Bárcenas,*[2] *Isaac C. Sanchez,*[3] *Ciro H. Ortiz-Estrada**[1]

The poly(1H,1H-dihydrofluorooctyl methacrylate) behavior in supercritical CO_2 was determined in relation to the emulsions formation phenomena in surfactants including a CO_2-philic chain and the particles formation process by RESS. The stability conditions show an obvious influence of both the polymer molecular weight and the CO_2 density, which are in competence with the thermal effect. The results are consistent with a LCST behavior in function of the molecular weight reaching the θ condition that converges for both the upper critical solution (UCSD) and the critical flocculation density (CFD) for a colloidal system. By using Sanchez-Lacombe equation of state, a solubility parameter is estimated and it confirms the affinity of the fluorinated polymer with CO_2, this in agreement with the literature information that relates surface tension with cohesion energy. In the particles formation by RESS, it was determined that concentration, saturation degree and nozzle diameter have a direct influence on the particle morphology and size; meanwhile, temperature and pre-expansion pressure are variables used to tune of saturation degree dependent phase behavior. Results show that particles of 200–400 nm can be obtained when 1%wt polymer, homogeneous solution and 130 μm nozzle diameter are used. Under those conditions, the nucleation process and the particles growth and size during precipitation can be controlled; the mechanism is analyzed in relation to the phase behavior.

Keywords: particle formation; PFOMA; RESS; stability and phase behavior; supercritical CO_2

Introduction

In the last 20 years, the development of new materials has motivated the use of supercritical technology due to its characteristics of operation conditions that allows one to tune-in the required properties. Applications where the particle morphology and size have a great significance in the product quality include polymers synthesis and processing, nanomaterials formation, biomaterials processing, and pharmaceutical products encapsulation.[1–11] In most of these processes, supercritical carbon dioxide ($scCO_2$) is selected.

Supercritical CO_2 is used due to its ability to promptly vary its solvent strength and, hence, the supersaturation and nucleation of dissolved compounds. This fact is an essential feature for the particle formation technology. An alternative for microparticle formation that takes advantage of supercritical fluid technology is the Rapid Expansion of Supercritical Solutions (RESS).[12,13] Here typically a polymer (or other molecule) is dissolved in a supercritical solvent, then the solution is expanded to ambient pressure through a nozzle of small (20–200 μm) diameter causing a sudden decrease in the solvent solubility and consequently the polymer

[1] Departamento de Ingeniería y Ciencias Químicas and Dirección de Investigación, Universidad Iberoamericana, Prol. Paseo de la Reforma 880, Lomas de Santa Fe, D. F. 01219 México
E-mail: ciro.ortiz@uia.mx
[2] Polymer and Biopolymer Research Group, CINVESTAV Querétaro, Quéretaro, Qro. 76230 México
[3] Chemical Engineering Department, University of Texas at Austin, Austin TX 78712 USA

precipitation. This expansion takes place in order of 10^{-5} s giving place to products with unique morphologies such as microspheres and fibers.[7,12–20] The most important RESS characteristics are the possibility to obtain a solvent-free product, and to control the particle distribution, size, and morphology by tuning the operation conditions (temperature, pressure, concentration), the thermodynamic state of the solution in the pre-expansion step (saturation degree), and the nozzle geometry.

CO_2 is a non-polar component with a low solvent strength; it does not solubilize many of the lipophilic or hydrophilic compounds used in the pharmaceutical and polymeric materials fields. Some soluble *''CO_2-philic''* compounds include fluorinated polymers that have been used in both microparticles formation by RESS[14,17,18,21–23] and as surfactants in colloidal dispersions studies, including emulsion[24–35] and dispersion.[36–45]

An adequate selection of a surfactant for dispersing components either lipophilic or hydrophilic in CO_2 is a technological opportunity for development of microemulsions, emulsions, and latexes that are used in diverse industrial processes applications. Particularly, perfluorinated surfactants are used to form water-in-scCO_2 microemulsions for protein and ionic compounds solvation.[25,46] In addition, nucleophilic displacement reactions leaded by either emulsions or microemulsions have shown greater reaction rates and yields when compared with conventional reactions in microemulsions of water in oil.[47,48]

At high enough CO_2 densities, the polymers can solvate and adopt an extended chain conformation; in contrast, at low densities and constant temperature, the solvent molecules expand from the monomer segment resulting in an increase in the monomer–monomer interactions and subsequently the chain collapses.[49–51] The density in which a chain collapses relates to the Upper Critical Solution Density (UCSD)[50,51] that is analogous to the LCST (Lower Critical Solution Temperature). CO_2's compressibility makes it possible to adjust its solvent strength through temperature or pressure changes in such a way that, above the UCSD, the polymer remains soluble in CO_2 at all proportions. When either the pressure or the density decreases, the system separates in two phases due to the difference between the polymer and the CO_2 free volume and compressibility. In colloidal stabilization, a Critical Flocculation Density (CFD) is defined as the density where the stabilizing chain collapses leading to particle-particle flocculation and agglomeration.[50]

Previously the critical flocculation density (CFD), that is, the CO2 density below which flocculation occurs, was determined to coincide with the upper critical solution density (UCSD) on the bulk phase diagram for a binary system composed of a stabilizer block and solvent.[35] Additionally, the UCSD coincided with the coil–globule transition density, where a single stabilizer block collapses in the solvent.[50] The predicted analogy between bulk phase separation and colloid flocculation is useful for designing surfactants for steric stabilization, given the large data base for polymer phase behavior.

Bulk polymer solubility knowledge is necessary for the design of all the above applications where separation using a supercritical solvent is involved. The most demanded applications are those that comprise particles formation that require a rapid and reliable determination of the solubility.[7,14,16,17,20,21,23,52] It is equally important in the study of surfactants to know the solvation-flocculation limits related with the bulk phase behavior and the CO_2-philic chain behavior.[24,20,30,35,43,53] The spirit of this paper is to further the understanding of bulk polymer behavior in scCO_2 that will shed light in phase behavior and stability of both bulk and colloidal systems.

It is reported that the solubility of a polymer in supercritical CO_2 is related to the surface tension of the pure polymer,[54] which, in turn, is with the cohesion energy density (CED). By using a solubility parameter approach, the polymer-solvent

interactions can be calculated from pure component information.

CED is directly related to de solubility parameter, δ, a property widely used in solubility estimations of several liquid solutions. The connection between solubility parameters of two materials characterizes the solubility effect between them.

The correlation between polymer-solvent solubility parameters is a measurement of the solution compatibility that, related to the Flory parameter, χ, is equal to:[55]

$$\chi = \frac{v_s}{RT}(\delta_S - \delta_P)^2 \quad (1)$$

where S is the solvent and P is the polymer.

The solubility parameter of the CO_2 is adjusted to 80%, taking into account that its quadrupole-quadrupole interactions are 20% of its solubility parameter.[55] The quadrupole moment has a greater influence over the interactions between two CO_2 molecules than between CO_2-polymer molecules.

A criterion for defining a good solvent for a given polymer is that the solvent-polymer solubility parameters be similar, i.e. χ approximating zero. When increasing the difference between parameters, the solution is expected to be unstable, resulting in an incompatible mixture and, hence, solution immiscibility. Even though Flory-Huggins equation does not give an exact description thermodynamic properties of the real polymeric solutions, it is a relatively simple theory that includes many of the essential characteristics of the macromolecules behavior in solution as is well documented in the literature.

Theoretically, CED can be determined from, say Sanchez-Lacombe Model[56–58] (S-L), calculated from the characteristic S-L parameters:

$$CED = P^*\tilde{\rho}^2 \quad (2)$$

and from the solubility parameter,

$$\delta = \sqrt{CED} = \tilde{\rho}\sqrt{P^*} \quad (3)$$

The S-L characteristic parameters can obtained for polymers from PvT data over a wide temperature and pressure ranges.

Fluorinated polymers exhibit the lowest surface tension among most commercial polymers and it is expected that its solubility parameter is close to that of $scCO_2$. In this work, our objective is to study poly(1H,1H-perfloroctyl methacrylate) (PFOMA), as a *''CO_2 -philic''* molecule, to determine bulk phase behavior (LCST and UCSD) in $scCO_2$. Additionally, the bulk phase behavior is exploited for particle formation design in $scCO_2$ by the RESS process. Our study focuses on the effect of solution concentration, operating temperature, saturation degree and nozzle diameter for particle size and morphology control. The above studies will help further the understanding of colloidal stability in $scCO_2$.

Experimental Part

Solutions of PFOMA with molecular weights ranging from 5.6 KDa to 110 KDa were prepared in $scCO_2$ at different temperatures and pressures. The experimental determination of the cloud point was determined by turbidimetry as described elsewhere.[34,59] The studied conditions (in equilibrium as well as in the RESS pre-expansion) were: 30–60 °C, 7–25 MPa, and 1–20% polymer weight. RESS's expansion nozzle diameters vary from 130–794 μm.

Taking into account the results of the phase behavior, the pre-expansion pressure was adjusted in such way that the solutions were in one of the following saturation degrees: homogeneous, saturated or supersaturated. The post-expansion conditions were those of the ambient (23–25 °C and 0.07 MPa).

Materials

The PFOMA was synthesized by atomic transfer radical polimerization (ATRP).[60] The carbon dioxide purity was 99.9% weight (grade 3) and it was purchased from Air Products, Mexico.

The chemical structure of the polymer is presented in Figure 1. The structural unit

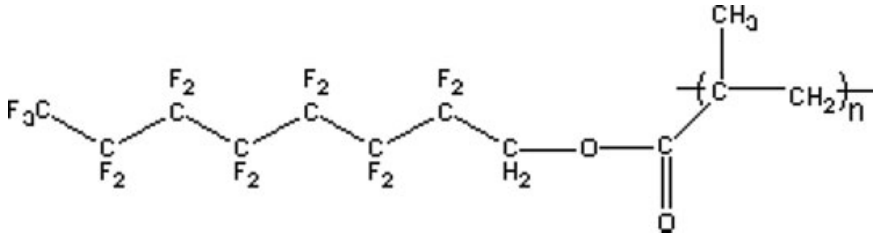

Figure 1.
Chemical structure of poly(1H,1H-dihydrofluorooctyl Methacrylate).

is similar to the poly(methyl metha acrylate) but instead of the methyl group it has an eight carbon chain with all the carbon atoms, except the first, saturated with fluorine.

PvT Data

The polymer's specific volume was measured with a PvT equipment (Gnomix Research).[61] The PvT data were determined in a temperature range of 30–200 °C with 10–20° steps and a 10–200 MPa pressure span.

Phase Behavior Measurement

The device used consists of a high-pressure cell, a temperature and pressure control, and an *in-line* spectrophotometer. Figure 2 shows the experimental apparatus.

The cell is a 316 SS cylinder with two lateral and one frontal holes where sapphire glasses are attached to allow the passage of a light beam through the lateral windows and direct visual observation on the frontal one. The temperature control was attained (±1 °C) with a thermo-circulator (Cole-Palmer) that had a thermostat. The pressure control was done with a high-pressure piston generator (HIP^R) and a transductor (Sensotec^R). Pressure is monitored throughout all experiments. The system for measuring the solution cloud point and turbidity consists of a light lamp (Ocean Optics^R) and a computer-coupled spectrometer (Ocean Optics^R).

The pressure was held high enough to assure that PFOMA-scCO_2 system remain in solution. Subsequently, the pressure was gradually reduced stepwise to reach equilibrium at each pressure. The solution was typically left stand for a period of 35–45 min, then the transmittance was recorded. Pressure was slightly raised and then slowly reduced to the target pressure to assure repeatability (±0.15 MPa). A minimum of two transmittance readings were recorded at each pressure. These gradual pressure reduction/increase

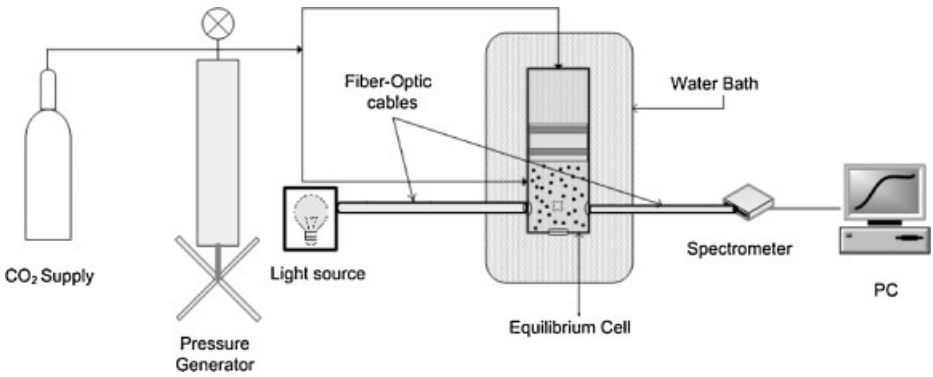

Figure 2.
Schematic diagram of the device for cloud point determination by turbidimetry.

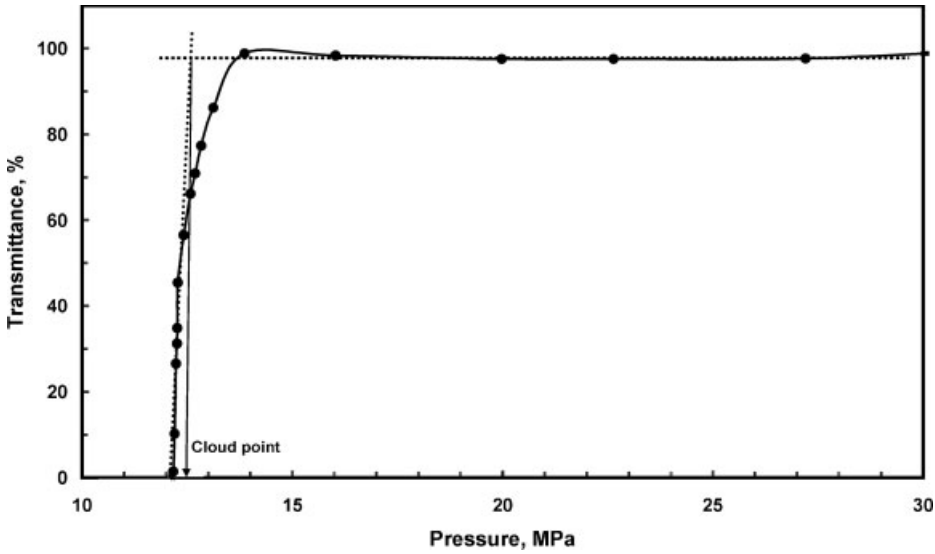

Figure 3.
Determination of cloud point at 110k, 30 °C and 20% wt. PFOMA.

continued until the solution became opaque (0%T). A cloud point pressure (P_{cp}) is defined as the system's pressure where the transmittance is 90% of the initial one (homogeneous solution). A typical cloud point curve is shown in Figure 3 for a 20 wt% PFOMA in $scCO_2$ solution (PFOMA mol. wt., 110 KDa) at 30 °C.

Particle Size Determination by RESS

The equipment used was adapted from the one employed in the equilibrium measurements (Figure 4). The system configuration comprises a solubilization and expantion unit.

The solubilization unit is the high-pressure cell described previously for the solubility determination. The unit comprises chromatographic capillaries (Agilent^R) with different internal diameters, an expansion valve and a container to collect the particles after the expansion.

The two units are connected from the high-pressure cell frontal cap to the valve that holds the capillary. A heating tape is employed to keep the temperature constant from the cell

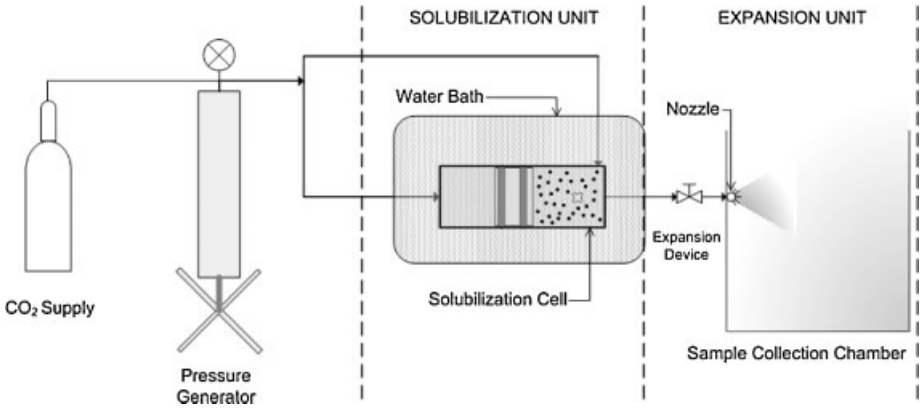

Figure 4.
Schematic diagram of the device empolyed for particles obtention by RESS.

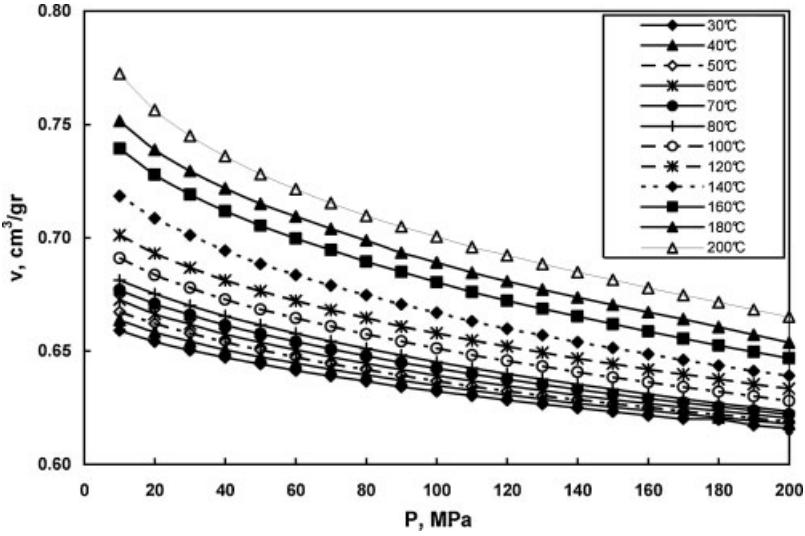

Figure 5.
PvT diagram of PFOMA (MW = 110 KDa).

to the expansion device. The sample particle was collected for SEM imaging (Phillips ESEM). SEM analysis includes particle size measurement with the built-in imaging software. A minimum of 100 particles were measured to within ±10%.

With the purpose of manipulating the pre-expansion conditions at a given fixed temperature, the experimental phase behavior, as determined above, helps designing precipitation pathways. This way allows manipulating solely the pressure to induce precipitation and particle formation.

Three saturation degrees ($S = P_{pre\text{-}exp}/P_{cp}$) were studied:

1. homogeneous, system's pressure above P_{cp} ($S > 1$),
2. saturated, pressure close to P_{cp} ($S \approx 1$), and
3. supersaturated, under the saturation pressure ($S < 1$).

Results and Discussion

PvT Measurements

PFOMA (110 KDa) PvT data are included in the Figure 5 (PvT data for other molecular weight PFOMA samples were also determined). PvT measurements for PFOMA of 60 KDa and 110 KDa were used to adjust the characteristic parameters of the Sanchez-Lacombe (S-L) equation, and are shown in Table 1.

Notice that the S-L parameters results are similar among the different molecular weights for both the entire data and the interest region (low temperature); therefore, a significant effect of the variation of molecular weight was not observed.

Table 1.
Characteristic parameters of the Sanchez-Lacombe equation adjusted with the PFMOA PvT data.

MW, k	N_{dat}	Intervale		P^*, MPa	T^*, K	ρ^*, kg/m^3
		T, °C	P, MPa			
60	240	30–200	10–200	348.1	566.69	1656.28
110	240			345.8	540.01	1676.98
60	100	30–70	10–200	348.2	534.21	1670.47
110	100			340.8	542.73	1659.09

Table 2.
Solubility parameters for PFOMA, PFOA, PMMA and CO_2, estimated by the S-L equation.

Polymer	$\delta(MPa)^{1/2}$
PFOMA	
60 k	17.1
110 k	16.9
Mean	**17.0**
PFOA	18.0
PMMA	21.3
CO_2	12.3*

*at 30 °C and 12.2 MPa.

Table 2 shows the comparison of δ for both PFMOA, the poly(1,1–dihydrofluorooctyl acrylate) (PFOA), the poly(methyl acrylate) (PMMA) and the CO_2.

The δ_{CO2} value obtained here was consistent with the previously reported value for the same conditions[62] (15.3 $MPa^{1/2}$). If we take into account that, as mentioned before, there is an extra 20% attributed to the $scCO_2$ quadrupole moment, the contribution from dispersion would be 12.2 $MPa^{1/2}$, which is close to our prediction. For the δ_{PMMA}, it is reported an experimental value of 22.1 $MPa^{1/2}$ [63] which also is consistent with the S-L prediction.

It is noteworthy from Table 2 that PFOMA has the closest δ value to those of $scCO_2$ (30 °C, 12.2 MPa) followed by PFOA indicating that both fluorinated polymers should be soluble in $scCO_2$ the phase behavior should be very similar.[61] On the other hand, the larger difference of δ's $scCO_2$ with respect to PMMA indicates that a mixture is immiscible.

It has been reported that polymers with smaller surface tension are more soluble in CO_2, due to the small polarizability of the latter that causes its dispersion contribution to CED to be lower.[54] Fluorinated polymers exhibit the lowest surface tension of most commercial polymers. For example, at 20 °C the surface tension of poly(1,1-dihidrodecafluoooctyl acrylate) is 10 mN/m, of the poly(1,2-dihidroheptafluorobutyl arylate) is 15 mN/m and of the PMMA is 41.1 mN/m.[54] This experimental observation correlates well with the solubility parameter approach describe above.

PFOMA-CO2 Phase Behavior

Figure 6 shows the pressure *versus* polymer concentration behavior of 5.6 KDa and 110 KDa for PFOMA in $scCO_2$. At all concentrations and temperatures, the cloud point pressure decreases with a decrease on

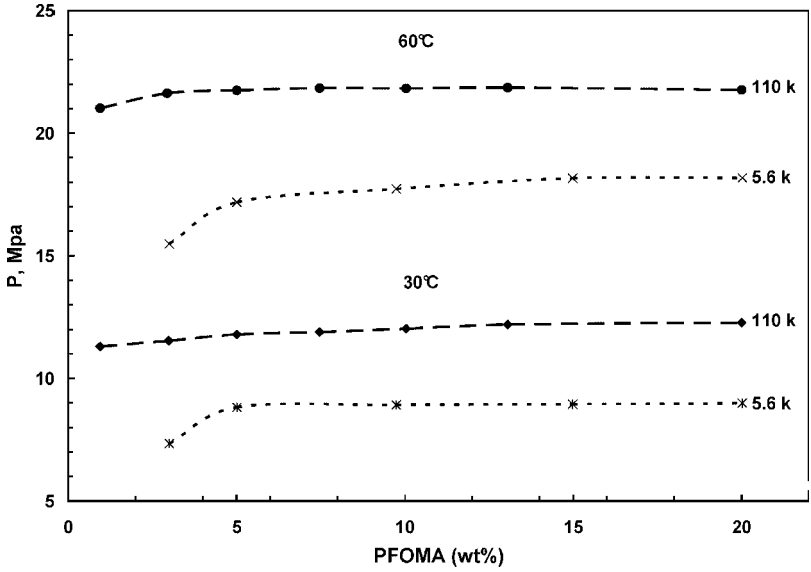

Figure 6.
Cloud point diagram at different temperatures for molecular weights of 5.6 and 110 k.

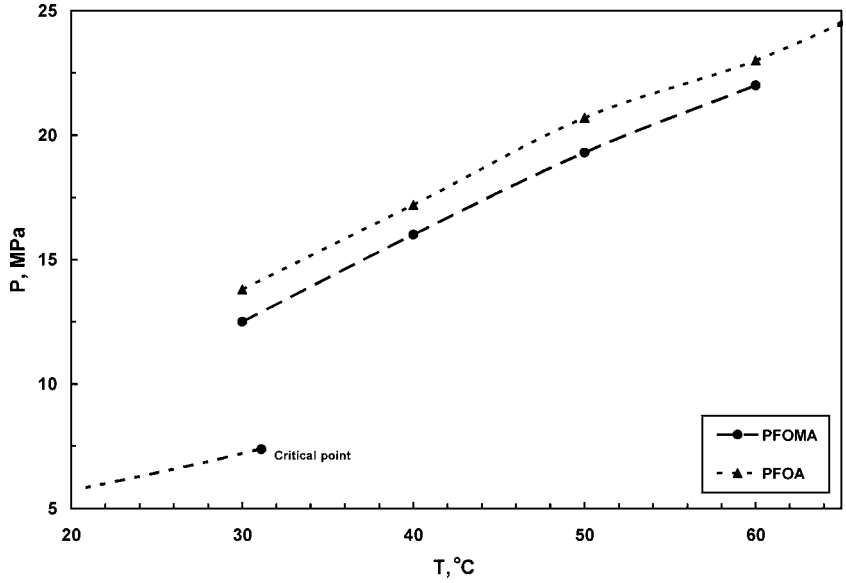

Figure 7.
LCST curve of PFOMA and PFOA in supercritical CO_2 ate the θ point. The pointed line indicates the vapor pressure curve of pure CO_2 at the critical point.

the polymer molecular weight, meaning that the polymer solubility increases on decreasing its molecular weight, as detailed in Figure 6.

Note that for concentrations above 5 wt.% the P_{cp} does not vary significantly. However, a maximum P_{cp} is close to 15 wt%. This condition defines the LCST of the solution. Extrapolations were performed to infinite molecular weight to determine the θ point of the solution for both PFOMA and PFOA.[61]

Figure 7 shows the LCST curves of PFOMA and PFOA[61] in a region close to the CO_2 critical point.[14,17,21,61] Notice that PFOA solutions require greater pressures than those of PFOMA to form a homogeneous solution; this is because PFOMA is well solvated by CO_2 at lower T,P,x conditions as predicted by their solubility parameters (see Table 2).

The corresponding density of the LCST point is called the upper-critical solution density (UCSD). At the UCSD, phase separation between the polymer chains and solvent is observed, and this entropically driven phenomenon is analogous to the lower critical solution temperature. In a colloidal system, the critical flocculation density (CFD) is the CO2 density below which flocculation occurs. It was previously determined that the CFD coincides with the upper critical solution density (UCSD) on the bulk phase diagram for a binary system composed of a stabilizer block and solvent.[35,50] This simple and elegant analogy has been proven useful in colloidal stability and nanoparticle formation.[34,35,64]

Figure 8 shows a comparison of the bulk UCSD (this study) behavior and those of Dickson, et al.[35] for a colloidal CFD behavior. CFD decreases when the temperature increases implying that lower CO_2 densities are required to stabilize the emulsion, this is consistent with the bulk results (UCSD). Nevertheless, the emulsion stability at lower densities was obtained at high molecular weights that are close to the θ density (Figure 8) where the CFD tends to approximate to the UCSD at higher molecular weights. This is due to the fact that long chains stabilize more rapidly the micelle interactions between its hydrophilic and CO_2-philic portions, requiring larger PFOMA chain.

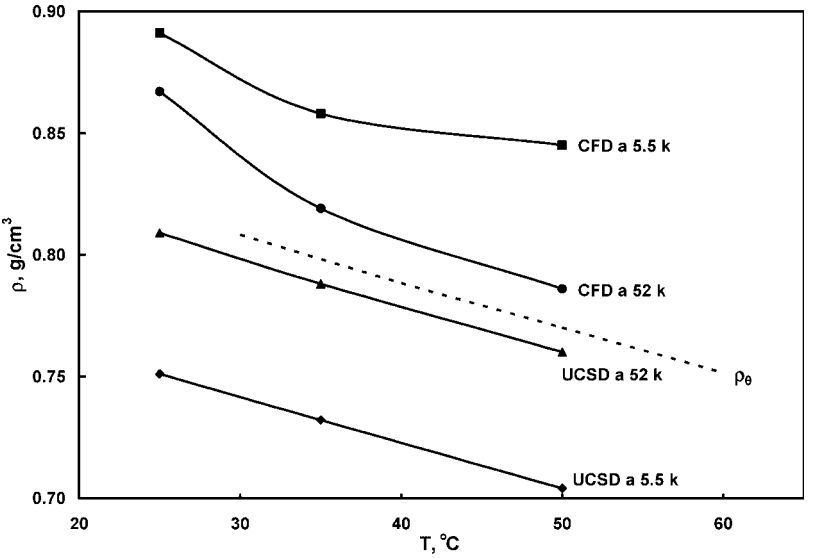

Figure 8.
Behavior of CFD[35] and UCSD of PFOMA at different molecular weights in comparison with density.

Particles Formation by RESS

The particle morphology and diameter were analyzed in function of: concentration, temperature, nozzle diameter and saturation degree.

Concentration

Concentration had a significant effect in particle morphology and diameter as shown in Figure 9. At a 20% concentration, the particles were completely amorphous and larger than 5 μm with a wide distribution of sizes. On the other hand, at 5% and 1% concentrations, the particles were smaller than 2 μm with a spherical morphologies and a narrow size distribution. In the present study, only solutions with 1% and 5% concentrations were investigated due to their more interesting characteristics. Notice that the particles with smaller size were obtained at 1% concentrations. It is observed that the concentration affects from a direct way to the morphology, being obtained amorphous particles and of great size to high concentration and defined and smaller spherical particles to low concentration.

Temperature

Table 3 displays the fact that temperature has not much influence on the particle diameter and morphology. For 5% solutions, it was detected that there is a light trend of diminishing the particle diameter when increasing the temperature at a constant nozzle size, the particles diameter were between 0.4–0.8 μm with regular spherical morphologies. The same effect was noticed at a 1% concentration having also well defined spherical particles but smaller sizes (0.3–0.6 μm).

The results indicate that one doesn't have a significant effect of the conditions of pre-expansion temperature (in consequence the pressure) on the morphology and size of the particle.

Nozzle Diameter

The nozzle diameter influences strongly in the size of independent particle to the temperature-pressure, considering that the solution is to PFOMA concentration of 1 and 5% and in homogeneous state. Figure 10 presents SEM results at different nozzle diameters and a 1% concentration. The difference in size is significant as the nozzle diameter increases.

For a nozzle diameter of 794 μm, the average particle size was 0.9 μm; for 250–500 μm, the particles were between

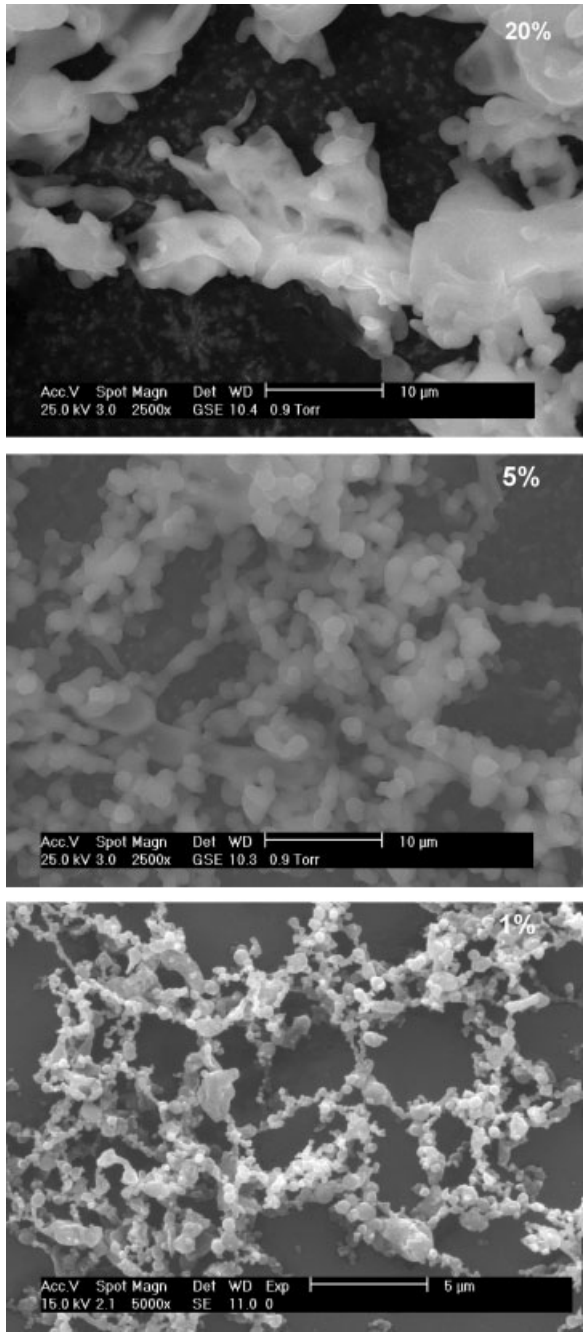

Figure 9.
Effect of the concentration. Homogeneous solution before the expansion.

0.4–0.6 μm; and for 130–180 μm, 0.2–0.4 μm. Here, nanometric materials were obtained. The same behavior was true for the 5% solution. Figure 11 shows the trend that the particle size follows with the variation of the nozzle diameter for both concentrations.

Table 3.
Effect of temperature in PFOMA particle size. Pre-expansion condition: homogeneous solution.

T, °C	%PFOMA	d_i, μm	d_p, μm	Particle morphology
40	5	500	0.8	Globular and ovoid
60			0.7	Globular and ovoid.
40		130	0.5	Globular
60			0.4	Globular
40	1	500	0.5	Globular
60			0.6	Globular,
40		130	0.4	Globular
60			0.3	Globular

* d_i, nozzle diameter; d_p, average particle diameter.

Saturation Degree

One of the variables that shows a direct dependence to the size and morphology of the precipitate one is the saturation degree.[17,65] The proposed saturation degree was established in terms of the ratio of the pre-expansion pressure to the cloud point pressure ($S = P/P_{sat}$) at the operation temperature. For $S > 1.05$, the solution is considered homogeneous; for $1.05 > S > 0.95$, saturated; and for $0.95 > S$ supersaturated. This criterion was defined with basis on the binodal-spinodal behavior observed in the turbidimetry results when the phase behavior study was done.[59]

In the SEM results shown in Figure 13, it is revealed a significant change in the particle size when varying the saturation degree. In general, when employing homogeneous solutions, particles with sizes under one micra and up to 0.4 μm and a narrow size distribution are obtained. In contrast, particles with a 1–5 μm size range are obtained with saturated solutions. For supersaturated solutions, few spherical and small particles were obtained, actually amorphous particles with an average 15 μm size predominated.

Figure 13 the tendency of the particle diameter is presented with the saturation grade, S. Notices that in the saturation area an abrupt change is presented in the behavior of the particle size due to the existence of the nucleation stage that is sensitive to the process of transition of phase of the stable state (going by the curve binodal) to the unstable one (spinodal). This has been observed in this study from the turbidimetry that will be analyzed later on.

In Figure 13 it is seen that small particles were obtained at S values above 1.3, establishes a limit for obtain micro-particles, reason why the pre-expansion pressure needs not to be further increased, avoiding a greater energetical effort.

Final Analysis

Concentration

The results obtained show an important effect of concentration on the particles morphology and size. This is consistent with literature where it is described that a decrease in concentration goes together with a reduction in the particle size and morphology changes.[14,15,21,65,66] Mawson et al.[14] studied the effect of concentration on particles size, recognizing that a concentration increase from 0.5 to 2% in the solution makes the particles size larger. Aniedobe y Thies[15] described that, for concentrations greater than 1%, agglomerated powders were obtained; for 15% concentrations, the morphology consisted of continuous fibers, with few microparticles observed. Chernyak et al.[21] concluded that increasing the concentration gives as a result an increase in the average particle size. Lele y Shine[65] pointed out that the changes in concentration affect the precipitate morphology since at a 0.263% concentration large fibers were obtained while a 0.08% solution resulted in fie powders. Tom y Debenedetti[66] estab-

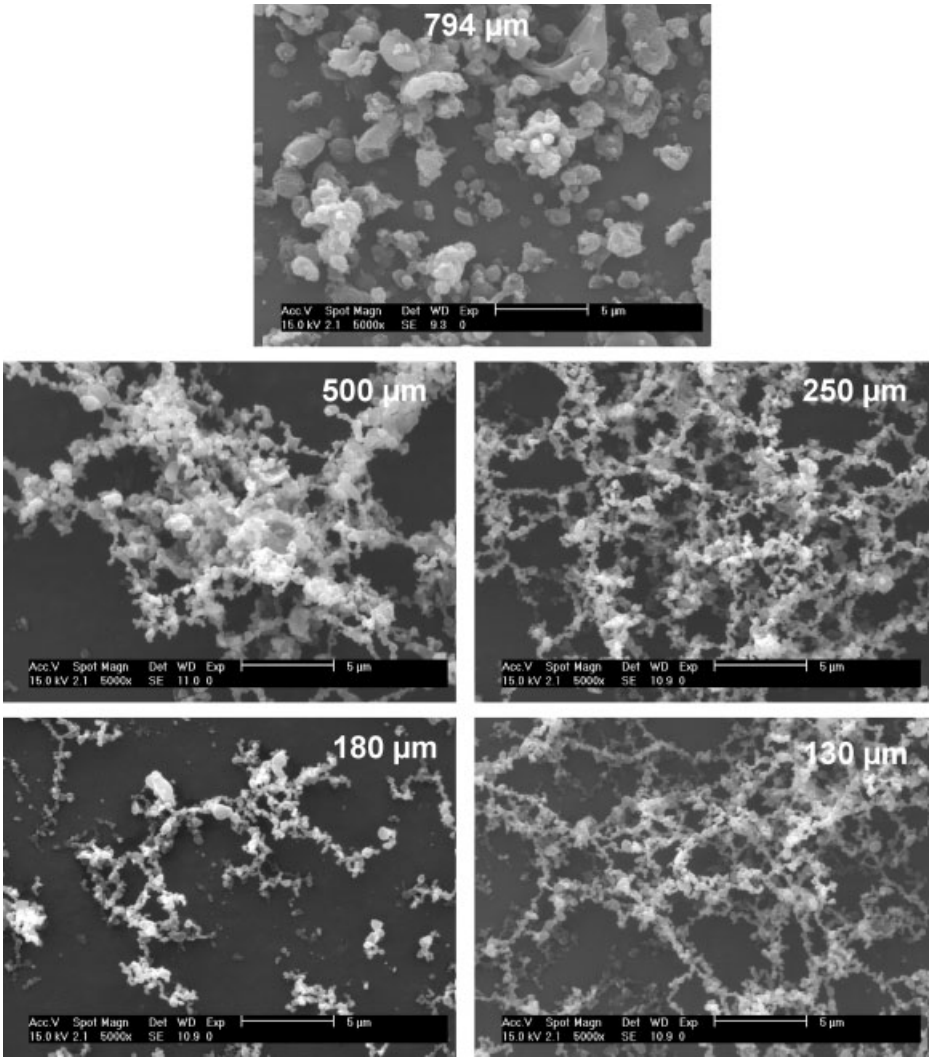

Figure 10.
Effect of the nozzle diameter to 1% concentration and 40 °C.

lished that, for concentrated solutions, the precipitate consisted in crystal needles of regular size with 10–120 μm; for diluted solutions the precipitate was disposed with both spherical and irregular particles of 4–10 μm sizes.

Concentration is related with the nucleation and particle growth phenomena. When an expansion at high concentration is performed, large volumes of polymer-rich phase are obtained, which favors the coalescence of particles nuclei during the solvent evaporation stage and, consequently, an increase in particles size. At low concentrations, the polymer-rich phase is isolated from the solvent-rich phase; therefore, the density of nucleating particles is small, preventing an effective coalescence and limiting the particles growth so small sizes and spherical structures are developed in the expansion-evaporation stage.[17]

Temperature

The difference between pre-expansion and equilibrium temperatures at the same

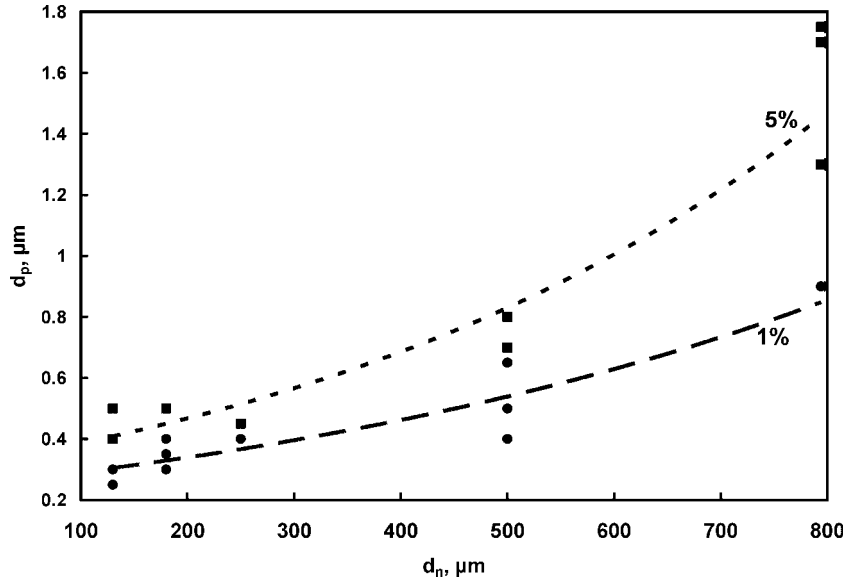

Figure 11.
Tendency in the effect of nozzle diameter on the size. The square points correspond to data to 5%, the circles to 1%.

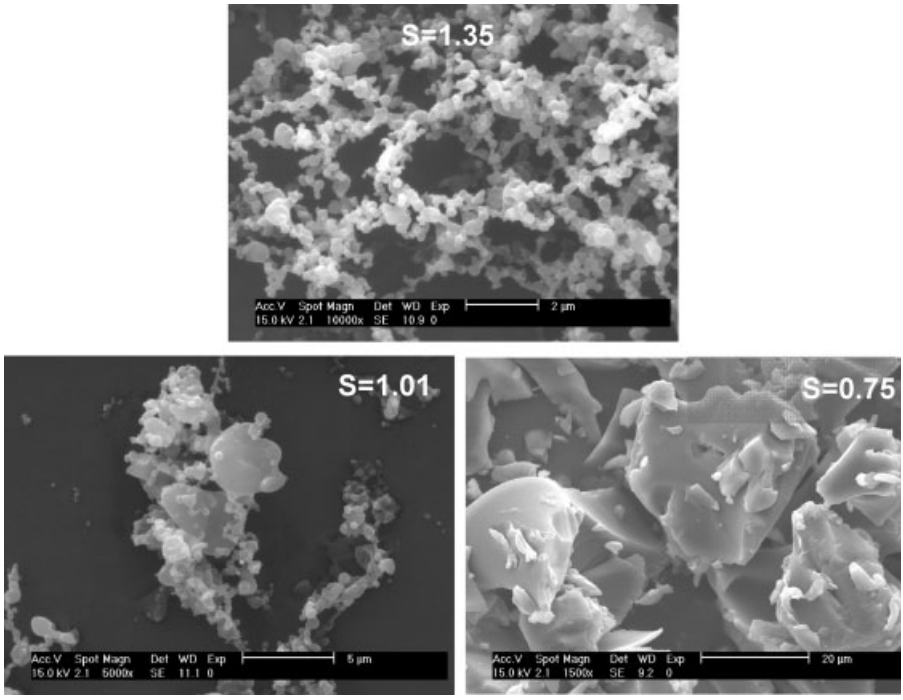

Figure 12.
SEM results to 1% concentration for different saturation grades, S.

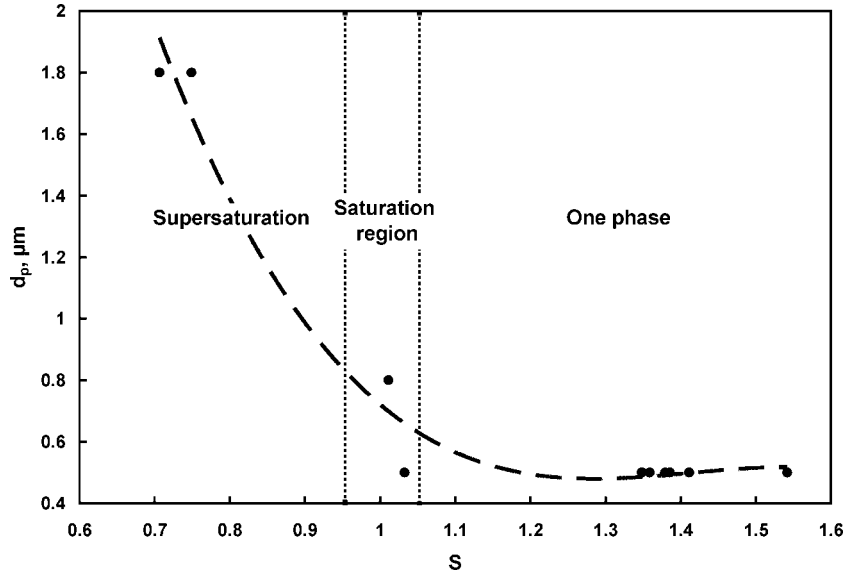

Figure 13.
Tendency in the particle size in relation to the saturation degree.

pressure and solution composition gives us a relative scale to induce phase separation. For systems with a LCST behavior, we have that, when the pre-expansion temperature is higher than the equilibrium one, the separation is thermally induced and the solution enters the nozzle as a mixture of two phases, this gives the solute more time to grow and form large particles by expantion.[67] On the other hand, the size of small diameter precipitates is generated when the pre-expantion temperature is below the equilibrium temperature, which causes the phase separation to occur from a homogeneous solution. In particular, Mawson et al.[14] showed that the pre-expansion temperature decreasing below the cloud point temperature directly leads to the precipitate particles size diminishment. In a similar way, Lele y Shine[65] reported a change in morphology from super-microscopic fibers to sub-microscopic particles when reducing the pre-expansion temperature. Debenedetti et al.[13] indicated that, theoreticaly, lowering the pre-expansion temperature under ideal conditions promotes the creation of small particles; nevertheless, in some studies it was found that an increase in the particle size[21] or in the pre-expansion temperature results in a decrease in particles size.[68]

Even when the temperature and pressure are variables that modify the characteristics of the precipitate due mainly to the saturation degree control and its influence in the equilibrium condition or phase stability by concentration, these do not contribute appreciably on the particles size and morphology by themselves but through the mentioned conditions. It has been shown that small changes in the pre-expansion pressure don't affect the the precipitate characteristics.[16,69] Alessi el al.[70] realized changes in the saturation pressure from 130 to 150 bar and they found that the particles size was reduced from 7.5 to 6 μm. Blasig et al.[17] pointed out that the change in pressure and temperature without variation in the saturation degree or solution condition does not have any effect on the morphology or size of the product.

Nozzle Design

Among the various factors that influence the precipitate morphology, it is believed that the nozzle design is of great importance. In the majority of experiments, the supercritical solution flows through a per-

forated hole[14,69] or a capillary tube.[65,67] The general tendency seems to indicate that the precipitate morphology depends more on the longitude to diameter ratio (L/D) and the nozzle diameter. Chernyak et al.[21] found that with a L/D of 165 bigger particles are obtained than with a L/D of 73, both with a 150 μm capillary. Alessi et al.[70] employed nozzles with L/D values in the range of 6–20 and diameters of 30 and 100 μm and determinate that the average particle size for both diamaters were 4.1 and 7.5 μm respectively, showing the effect of reducing the nozzle diameter in the particle size. Charoenchaitrakool et al.[16] observed that varying the capillary longitude from 1 to 2 cm with a constant nozzle diameter of 50 μm does not have a significant effect on the product size. In our case it is observed a similar tendency of reducing the particle size when decreasing the nozzle diameter, having obtained particles that decrease in size (clearly following this tendency) from 2 μm to 200 nm (nanometric scale).

Saturation Degree

One of the variables that have a direct influence on the precipitate characteristics is the saturation degree of a solution during the pre-expansion stage. Blasig et al.[17] determinated that the saturation degree has a significant effect on the final product morphology, they defined the saturation degree as the ratio of the pre-expansion concentration to the equilibrium concentration at the same temperature and pressure of the pre-expansion zone. At insaturated conditions, particles size in the submicron range are obtained while at saturated conditions the size lays in the micron range and with supersaturated solutions the particles size is increased.

Lele y Shine[65] related the saturation degree with the reduction of solution density or the time scale required for the phases separation in solutions that have LCST behavior. The particles formation depends on the path followed on the cross point of the cloud points curve. In fact, they observed that when the pre-expansion conditions are above the cloud point (homogeneous phase) the particles obtained are 0.2 to 0.6 μm in size because there is not enough time for growth and deformation since the cross point in the cloud point curve is right in the nozzle exit. The whole process occurs in a 10 second time scale. In general, for a solution with LCST behavior, a decrease in pressure, increase on temperature or increase in concentration can cause a cross point in the equilibrium curve within the pre-expansion region, changing the saturation degree and the residence time of the solution in the nozzle.

Mechanism

The saturation degree indicates us the type of morphology that is expected with basis in the path of the RESS process chosen. Cherniyak et al.[21] discuss the particle formation process basing on the nucleation and growth theory. From the thermodynamic point of view, the nozzle expansion is a transfer process of the polymer/solvent system from one to two phases, going through the states originated by the simultaneous falls of pressure and temperature. These falls are due to the expansion from the cross point of the binodal curve to the metastable region of the spinodal curve where the solution reaches supersaturation and, hence, starts the process of nucleation where finally reaches the two phases region.

Huang and Moriyoshi[19] proposed a possible micronization mechanism in relation to a special nozzle design. They indicated that the particle formation befins with its nucleation and growth in the nozzle with a subsequent expansion of the solution and a breakage that generates fine drops and secondary evaporation to finally lead to the sub-micrometric particles creation.

A similar mechanism has been discussed by Weber y Thies[71] who propose a nucleation-condensation-coagulation model pointing toward particles being shaped due to an abrupt increase in supersaturation during expansion followed by growth caused by coagulation in the nozzle outlet as a result of several mechanisms. They demonstrate that the typical time that

the particles take to growth from 10 nm to micrometric levels fluctuates from 10 to hundreds of seconds if the growth is attributable to coagulation due to Brownian motion.

With the aim of analyzing the mechanism of nucleation previous to expansion due to the supersaturation of the solution by pressure reduction, the growth of particles in the polymer-rich phase was determined by turbidimetry whilst measuring the cloud point.[59] By turbidimetry (see experimental section), there were generated the transmittance spectra during the pressure

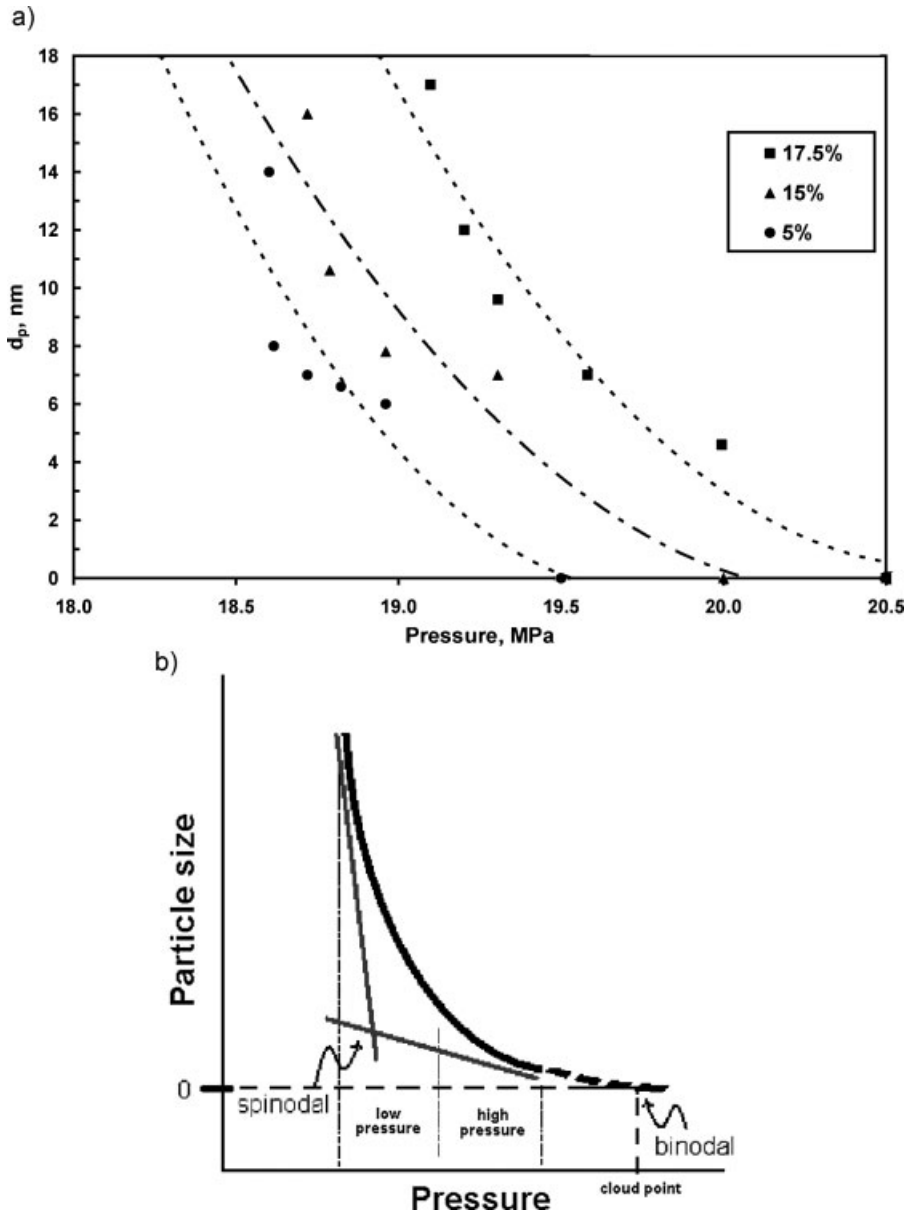

Figure 14.
Behavior in the growth of the particle of the dispersed phase during the PIPS process of the solution. Thermodynamic outline.

reduction tests and, via Mie's theory,[34,59] the particle diameter obtained by the presence of two phases was estimated. Here, the dispersed phase consists in the PFOMA particles precipitating in the bulk solution originating from high pressures and a homogeneous (one phase) solution.

Figure 14(a) shows the particle growth dynamics during decompression (PIPS), it is observed a curve with a light slope change from a homogeneous phase (high pressure) without precipitation to the growth of the dispersed phase (low pressure). Notice that in the pressure reduction stage the particles diameter was in the 2–20 nm range with an exponential growth where the total turbidity is reached and the particle size is larger. This phenomenon represents the nucleation process before the particles enter the nozzle during the expansion in the RESS process in the phase change path dominated by thermodynamics in the transition of the stable-metastable-supersaturation states.[72]

In our case, we are proposing that the spinodal point is denoted by the slope change during the particles growth that is where the system is unstable (see Figure 14b). These results show that the nucleation phase happens in the bulk solution and that the growth dynamics are completely dependent on the nozzle geometry in the coagulation and evaporation phase.

Conclusions

Knowledge of phase behavior in a polymer-CO_2 solution used as surfactant media for emulsions development is very relevant to understand the micelle conformation and its stability conditions as well as the dynamics of the particles formation process by RESS.

PFOMA-CO_2SC equilibrium experimental measurements shows the influence of the molecular weight of the polymer in the behavior LCST to the θ point. The effect of the CO_2 density in competition with the thermal effect. It is observed that the CFD approaches to the UCSD when the molecular weight of the PFOMA is increased converging in the θ density, because long chains stabilize the interactions of the micelle more quickly between the part hydrophilic and CO_2-philic chain.

The effect of solubility of the PFOMA in CO_2SC by solubility parameter estimate with S-L equation agreement sample with the experimental results, that it is an useful tool in the study of the polymer compatibility in CO_2SC.

It has been shown that it is possible to obtain PFOMA nanoparticles of 200–400 nm by RESS. Controlling the pre-expansion conditions with the saturation degree of the homogeneous solution, diluted concentrations (1% weight of PFOMA) and nozzle diameter of 130 μm.

The most influencing variables in particles morphology and size are: concentration, saturation degree and nozzle diameter. Temperature and pressure do not have a direct influence on the particles formation but are only used to tune the conditions by concentration and saturation degree that are determinate by phase behavior.

The nucleation mechanism as a first stage in the particles formation dynamics is observed to happen because of thermodynamic effects in the transition from the homogeneous phase towards the binodal curve, spinodal to supersaturation. The particle size during the expansion phenomena initially reaches 2–20 nm magnitudes in the binodal-spinodal region. Subsequently, particles grow to larger magnitudes due to supersaturation with the nucleation taking place before the particles exit the nozzle.

[1] M. Perrut, Supercritical Fluid Applications: Industrial Developments and Economic Issues. *Ind. Eng. Chem. Res.* **2000**, *39*, 4531–4535.
[2] E. Reverchon, G. Della Porta, I. De Rosa, P. Subra, D. Letourneur, Supercritical Antisolvent Micronización of Some Biopolymers. *J. Supercrit. Fluids* **2000**, *18*, 239. 245.
[3] A. S. Teja, C. A. Eckert, Commentary on Supercritical Fluids: Research and Applications. *Ind. Eng. Chem. Res.* **2000**, *39*, 4442–4444.

[4] A. I. Cooper, Recent Developments in Materials Synthesis and Processing Using Supercritical CO_2. *Adv. Mat.* **2001**, *13*, 1111–1114.
[5] N. Elvassore, M. Baggio, P. Pallado, A. Bertucco, Production of Different Morphologies of Biocompatible Polymeric Materials by Supercritical CO_2 Antisolvent Techniques. *Biotechnol. Bioeng.* **2001**, *73*, 449–457.
[6] J. Jung, M. Perrut, Particle Design Using Supercritical Fluids: Literature and Patent Survey. *J. Supercrit. Fluids* **2001**, *20*, 179–219.
[7] K. Matsuyama, K. Mishima, K.-I. Hayashi, H. Ishikawa, H. Matsuyama, T. Harada, Formation of Microcapsules of Medicines by the Rapid Expansion of a Supercritical Solution with a Nonsolvent. *J. App. Polymer Sci.* **2003**, *89*, 742–752.
[8] D. L. Tomasko, H. Li, D. Liu, X. Han, M. J. Wingert, L. J. Lee, K. W. Koelling, A Review of CO_2 Applications in the Processing of Polymers. *Ind. Eng. Chem. Res.* **2003**, *42*, 6431–6456.
[9] J. Fages, H. Lochard, J.-J. Letourneau, M. Sauceau, E. Rodier, Particle Generation for Pharmaceutical Applications Using Supercritical Fluid Technology. *Powder Tech.* **2004**, *141*, 219–226.
[10] S.-D. Yeo, E. Kiran, Formation of Polymer Particles with Supercritical Fluids: A review. *J. Supercrit. Fluids* **2005**, *34*, 287–308.
[11] E. Reverchon, R. Adami, Nanomaterials and Supercritical Fluids. *J. Supercrit. Fluids* **2006**, *37*, 1–22.
[12] D. W. Matson, J. L. Fulton, R. C. Petersen, R. D. Smith, Rapid Expansion of Supercritical Fluid Solutions: Solute Formation of Powders, Thin Films, and Fibers. *Ind. Eng. Chem. Res.* **1987**, *26*, 2298–2306.
[13] P. G. Debenedetti, J. W. Tom, X. Kwauk, S. D. Yeo, Rapid Expansion of Supercritical Solutions (RESS): Fundamentals and Applications. *Fluid Phase Equilibria* **1993**, *82*, 311–321.
[14] S. Mawson, K. P. Johnston, J. R. Combes, J. M. DeSimone, Formation of Poly(1,1,2,2-tetrahydroperfluorodecyl acrylate) Submicron Fibers and Particles from Supercritical Carbon Dioxide Solutions. *Macromolecules* **1995**, *28*, 3182–3191.
[15] N. E. Aniedobe, M. C. Thies, Formation of Cellulose Acetate Fibers by the Rapid Expansion of Supercritical Methanol Solutions. *Macromolecules* **1997**, *30*, 2792–2794.
[16] M. Charoenchaitrakool, F. Dehghani, N. R. Foster, H. K. Chan, Micronization by Rapid Expansion of Supercritical Solutions to Enhance the Dissolution Rates of Poorly Water-Soluble Pharmaceuticals. *Ind. Eng. Chem. Res.* **2000**, *39*, 4794–4802.
[17] A. Blasig, C. Shi, R. M. Enick, M. C. Thies, Effect of Concentration and Degree of Saturation on RESS of a CO2-Soluble Fluoropolymer. *Ind. Eng. Chem. Res.* **2002**, *41*, 4976–4983.
[18] M. J. Meziani, P. Pathak, W. Wang, T. Desai, A. Patil, Y.-P. Sun, Polymeric Nanofibers from Rapid Expansion of Supercritical Solution. *Ind. Eng. Chem. Res.* **2005**, *44*, 4594–4598.
[19] J. Huang, T. Moriyoshi, Fabrication of Fine Powders by RESS with a Clearance Nozzle. *J. Supercrit. Fluids* **2006**, *37*, 292–297.
[20] M. Türk, G. Upper, P. Hils, Formation of Composite Drug-polymer Particles by Co-precipitation During the Rapid Expansion of Supercritical Fluids. *J. Supercrit. Fluids* **2006**, *39*, 253–263.
[21] Y. Chernyak, F. Henon, R. B. Harris, R. D. Gould, R. K. Franklin, J. R. Edwards, J. M. DeSimone, R. G. Carbonell, Formation of Perfluoropolyether Coatings by the Rapid Expansion of Supercritical Solutions (RESS) Process. Part 1: Experimental Results. *Ind. Eng. Chem. Res.* **2001**, *40*, 6118–6126.
[22] R. K. Franklin, J. R. Edwards, Y. Chernyak, R. D. Gould, F. Henon, R. G. Carbonell, Formation of Perfluoropolyether Coatings by the Rapid Expansion of Supercritical Solutions (RESS) Process. Part 2: Numerical Modelling. *Ind. Eng. Chem. Res.* **2001**, *40*, 6127–6139.
[23] K. Matsuyama, K. Mishima, Coacervation Microencapsulation of Talc Particles with a Fluoropolymer by Pressure-Induced Phase Separation of Supercritical Carbon Dioxide Solutions. *Ind. Eng. Chem. Res.* **2006**, *45*, 6162–6168.
[24] K. L. Harrison, K. P. Johnston, I. C. Sanchez, Effect of Surfactants on the Interfacial Tension between Supercritical Carbon Dioxide and Polyethylene Glycol. *Langmuir* **1996**, *12*, 2637–2644.
[25] K. P. Johnston, K. L. Harrison, M. J. Clarke, S. M. Howdle, M. P. Heitz, F. V. Bright, C. Carlier, T. W. Randolph, Water-in-carbon Dioxide Microemulsions: an Environment for Hydrophiles Including Proteins. *Science* **1996**, *271*, 624–626.
[26] J. B. McClain, D. E. Betts, D. A. Canelas, E. T. Samulski, J. M. DeSimone, J. D. Londono, H. D. Cochran, G. D. Wignall, D. Chillura-Martino, R. Triolo, Design of Nonionic Surfactants for Supercritical Carbon Dioxide. *Science* **1996**, *274*, 2049–2051.
[27] M. L. O'Neill, M. Z. Yates, K. L. Harrision, K. P. Johnston, D. A. Canelas, E. E. Betts, J. M. DeSimone, S. P. Wilkinson, Emulsion Stabilization and Flocculation in CO_2. 1. Turbidimetry and tensiometry. *Macromolecules* **1997**, *30*, 5050–5059.
[28] E. J. Singley, W. Liu, E. J. Beckman, Phase Behavior and Emulsion Formation of Novel Fluoroether Amphiphiles in Carbon Dioxide. *Fluid Phase Equilibria* **1997**, *128*, 199–219.
[29] M. Z. Yates, M. L. O'Neill, K. P. Johnston, S. E. Webber, D. A. Canelas, D. E. Betts, J. M. DeSimone, Emulsion Stabilization and Flocculation in CO_2. 2. Dynamic Light Scattering. *Macromolecules* **1997**, *30*, 5060–5067.
[30] K. L. Harrison, S. R. P. da Rocha, M. Z. Yates, K. P. Johnston, D. Canelas, J. M. DeSimone, Interfacial Activity of Polymeric Surfactants at the

Polystyrene-Carbon Dioxide Interface. *Langmuir* **1998**, *14*, 6855–6863.
[31] C. T. Lee, P. A. Psathas, K. P. Johnston, J. deGrazia, T. W. Randolph, Water-in-Carbon Dioxide Emulsions: Formation and Stability. *Langmuir* **1999**, *15*, 6781–6791.
[32] P. A. Psathas, E. A. Sander, W. Ryoo, D. Mitchell, R. J. Lagow, K. T. Lim, K. P. Johnston, Interfacial Studies of the Formation of Microemulsions of Water in Carbon Dioxide with Fluorinated Surfactants. *J. Disp. Sci. Tech.* **2002**, *23*, 81–92.
[33] P. A. Psathas, E. A. Sander, M. Y. Lee, K. T. Lim, K. P. Johnston, Mapping the Stability and Curvature of Emulsions of H_2O and Supercritical CO_2 with Interfacial Tension Measurements. *J. Disp. Sci. Tech.* **2002**, *23*, 65–80.
[34] J. L. Dickson, P. A. Psathas, B. Salinas, C. Ortiz-Estrada, G. Luna-Barcenas, H. S. Hwang, K. T. Lim, K. P. Johnston, Formation and Growth of Water-in-CO_2 Miniemulsions. *Langmuir* **2003**, *19*, 4895–4904.
[35] J. L. Dickson, C. Ortiz-Estrada, J. F. J. Alvarado, H. S. Hwang, I. C. Sanchez, G. Luna-Barcenas, K. T. Lim, K. P. Johnston, Critical Flocculation Density of Dilute Water-in-CO_2 Emulsions Stabilized with Block Copolymers. *J. Colloid Interface Sci.* **2004**, *272*, 444–456.
[36] J. M. DeSimone, E. E. Maury, Y. Z. Menceloglu, J. B. McClain, T. J. Romack, J. R. Combes, Dispersion Polymerizations in Supercritical Carbon Dioxide. *Science* **1994**, *265*, 356–359.
[37] D. A. Canelas, D. E. Betts, J. M. DeSimone, Dispersion Polymerization of Styrene in Supercritical Carbon Dioxide: Importance of Effective Surfactants. *Macromolecules* **1996**, *29*, 2818–2821.
[38] C. Lepilleur, E. J. Beckman, Dispersion Polymerization of Methyl Methacrylate in Supercritical CO_2. *Macromolecules* **1997**, *30*, 745–756.
[39] D. A. Canelas, D. E. Betts, J. M. DeSimone, M. Z. Yates, K. P. Johnston, Poly(vinyl acetate) and Poly(vinyl acetate-co-ethylene) Latexes via Dispersion Polymerizations in Carbon Dioxide. *Macromolecules* **1998**, *31*, 6794–6805.
[40] T. Carson, J. Lizotte, J. M. Desimone, Dispersion Polymerization of 1-Vinyl-2-pyrrolidone in Supercritical Carbon Dioxide. *Macromolecules* **2000**, *33*, 1917–1920.
[41] M. R. Giles, S. J. O'Connor, J. N. Hay, R. J. Winder, S. M. Howdle, Novel Graft Stabilizers for the Free Radical Polymerization of Methyl Methacrylate in Supercritical Carbon Dioxide. *Macromolecules* **2000**, *33*, 1996–1999.
[42] G. Li, M. Z. Yates, K. P. Johnston, S. M. Howdle, In-Situ Investigation on the Mechanism of Dispersion Polymerization in Supercritical Carbon Dioxide. *Macromolecules* **2000**, *33*, 4008–4014.
[43] H. Shiho, J. M. Desimone, Dispersion Polymerization of Styrene in Supercritical Carbon Dioxide Utilizing Random Copolymers Containing a Fluorinated Acrylate for Preparing Micron-size Polystyrene Particles. *J. Polymer Sci., Part A: Polymer Chem.* **2000**, *38*, 1146–1153.
[44] H. Shiho, J. M. DeSimone, Dispersion Polymerization of Glycidyl Methacrylate in Supercritical Carbon Dioxide. *Macromolecules* **2001**, *34*, 1198–1203.
[45] H. Yuvaraj, H. S. Hwang, M. H. Woo, E. J. Park, H. S. Ganapathy, Y.-S. Gal, K. T. Lim, Dispersion Polymerization of Styrene in Supercritical CO_2 Stabilized by Random Copolymers of 1H,1H-perfluorooctyl Methacrylate and 2-Dimethylaminoethyl Methacrylate. *J. Supercrit. Fluids* **2007**, *42*, 359–365.
[46] M. J. Clarke, K. L. Harrison, K. P. Johnston, S. M. Howdle, Water in Supercritical Carbon Dioxide Microemulsions: Spectroscopic Investigation of a New Environment for Aqueous Inorganic Chemistry. *J. Am. Chem. Soc.* **1997**, *119*, 6399–6406.
[47] G. B. Jacobson, C. T. Lee, S. R. P. daRocha, K. P. Johnston, Organic Synthesis in Water/Carbon Dioxide Emulsions. *J. Org. Chem.* **1999**, *64*, 1207–1210.
[48] G. B. Jacobson, C. T. Lee, K. P. Johnston, Organic Synthesis in Water/Carbon Dioxide Microemulsions. *J. Org. Chem.* **1999**, *64*, 1201–1206.
[49] D. Chillura-Martino, R. Triolo, J. B. McClain, J. R. Combes, D. E. Betts, D. A. Canelas, J. M. DeSimone, E. T. Samulski, H. D. Cochran, D. Londono, G. D. Wignall, Neutron Scattering Characterization of Homopolymers and Graft-copolymer Micelles in Supercritical Carbon Dioxide. *J. Mol. Structure* **1996**, *383*, 3–10.
[50] J. C. Meredith, K. P. Johnston, Theory of Polymer Adsorption and Colloid Stabilization in Supercritical Fluids. 1. Homopolymer Stabilizers. *Macromolecules* **1998**, *31*, 5507–5517.
[51] G. Luna-Barcenas, J. C. Meredith, I. C. Sanchez, K. P. Johnston, D. G. Gromov, J. J. de Pablo, Relationship Between Polymer Chain Conformation and Phase Boundaries in a Supercritical Fluid. *J. Chem. Phys.* **1997**, *107*, 10782–10792.
[52] S. Palakodaty, P. York, Phase Behavioral Effects on Particle Formation Processes Using Supercritical Fluids. *Pharma. Res.* **1999**, *16*, 976–985.
[53] W. Ye, J. M. DeSimone, Synthesis of Sugar-containing Amphiphiles for Liquid and Supercritical Carbon Dioxide. *Ind. Eng. Chem. Res.* **2000**, *39*, 4564–4566.
[54] M. L. O'Neill, Q. Cao, M. Fang, K. P. Johnston, S. P. Wilkinson, C. D. Smith, J. L. Kerschner, S. H. Jureller, Solubility of Homopolymers and Copolymers in Carbon Dioxide. *Ind. Eng. Chem. Res.* **1998**, *37*, 3067–3079.
[55] J. M. Prausnitz, R. N. Lichtenthaler, E. G. de Azevedo, *Molecular Thermodynamics of Fluid-Phase Equilibria*, Prentice Hall, New Jersey, EUA 1999.
[56] I. C. Sanchez, R. H. Lacombe, An Elementary Molecular Theory of Classical Fluids. Pure Fluids. *J. Phys. Chem.* **1976**, *80*, 2352–2362.
[57] I. C. Sanchez, R. H. Lacombe, Statistical Thermodynamics of Polymer Solutions. *Macromolecules* **1978**, *11*, 1145–1156.
[58] I. C. Sanchez, R. H. Lacombe, Statistical Thermodynamics of Polymer Solutions. *Macromolecules* **1978**, *11*, 1145–1156.

[59] J. G. Santoyo-Arreola, *Formación de Partículas de PFOMA Mediante CO_2 Supercrítico*. MSc Thesis, Universidad Iberoamericana, México, **2006**.
[60] K. T. Lim, M. Y. Lee, M. J. Moon, G. D. Lee, S.-S. Hong, J. L. Dickson, K. P. Johnston, Synthesis and Properties of Semifluorinated Block Copolymers Containing Poly(ethylene oxide) and Poly(fluorooctyl methacrylates) via Atom Transfer Radical Polymerization. *Polymer* **2002**, *43*, 7043–7049.
[61] G. Luna-Barcenas, S. Mawson, S. Takishima, J. M. DeSimone, I. C. Sanchez, K. P. Johnston, Phase Behavior of Poly(1,1-dihydroperfluorooctylacrylate) in Supercritical Carbon Dioxide. *Fluid Phase Equilib.* **1998**, *146*, 325–337.
[62] K. P. Johnston, D. G. Peck, S. Kim, Modeling Supercritical Mixtures: How Predictive is it? *Ind. Eng. Chem. Res.* **1989**, *28*, 1115–1125.
[63] C. M. Hansen, *Hansen Solubility Parameters: A User's Handbook*, CRC, Boca Raton, Florida 2000.
[64] X. Lu, B. A. Korgel, K. P. Johnston, Synthesis of Germanium Nanocrystals in High Temperature Supercritical CO_2. *Nanotechnology* **2005**, *16*, S389–S39.
[65] A. K. Lele, A. D. Shine, Effect of RESS Dynamics on Polymer Morphology. *Ind. Eng. Chem. Res.* **1994**, *33*, 1476–1485.
[66] J. W. Tom, P. G. Debenedetti, Formation of Bioerodible Polymeric Microspheres and Microparticles by Rapid Expansion of Supercritical Solutions. *Biotechnol. Prog.* **1991**, *7*, 403–411.
[67] J. W. Tom, P. G. Debenedetti, Particle Formation with Supercritical Fluids -a Review. *J. Aerosol Sci.* **1991**, *22*, 555–584.
[68] J.-H. Kim, T. E. Paxton, D. L. Tomasko, Microencapsulation of Naproxen Using Rapid Expansion of Supercritical Solutions. *Biotechnol. Prog.* **1996**, *12*, 650–661.
[69] R. S. Mohamed, D. S. Halverson, P. G. Debenedetti, R. K. Prud'homme, Solids Formation After the Expansion of Supercritical Mixtures. in: *Supercritical Fluid Science and Technology*, K. P. Johnston, J. M. L. Penninger, Eds., ACS Symposium Series 406, Washington D.C. 1989.
[70] P. Alessi, A. Cortesi, I. Kikic, N. R. Foster, S. J. Macnaughton, I. Colombo, Particle Production of Steroid Drugs Using Supercritical Fluid Processing. *Ind. Eng. Chem. Res.* **1996**, *35*, 4718–4726.
[71] M. Weber, M. C. Thies, A Simplified and Generalized Model for the Rapid Expansion of Supercritical Solutions. *J. Supercrit. Fluids* **2007**, *40*, 402–419.
[72] C. H. Ortiz-Estrada, J. G. Santoyo-Arreola, G. Luna-Barcenas, I. C. Sanchez, Phase Transition and Stability of Polymers Solutions in Supercritical CO_2 by Turbidimetry. *Rev. Mex. Ing. Quim.* **2007**, *6*, 347–357.

